



# The Effect of a Simple Annealing Heat Treatment on the Mechanical Properties of Cold-Sprayed Aluminum

A.C. Hall, D.J. Cook, R.A. Neiser, T.J. Roemer, and D.A. Hirschfeld

(Submitted July 28, 2005; in revised form January 4, 2006)

Cold spray, a new member of the thermal spray process family, can be used to prepare dense, thick metal coatings. It has tremendous potential as a spray-forming process. However, it is well known that significant cold work occurs during the cold spray deposition process. This cold work results in hard coatings but relatively brittle bulk deposits. This work investigates the mechanical properties of cold-sprayed aluminum and the effect of annealing on those properties. Cold spray coatings approximately 1 cm thick were prepared using three different feedstock powders: Valimet H-10; Valimet H-20; and Brodmann Flomaster. ASTM E8 tensile specimens were machined from these coatings and tested using standard tensile testing procedures. Each material was tested in two conditions: as-sprayed; and after a 300 °C, 22 h air anneal. The as-sprayed material showed high ultimate strength and low ductility, with <1% elongation. The annealed samples showed a reduction in ultimate strength but a dramatic increase in ductility, with up to 10% elongation. The annealed samples exhibited mechanical properties that were similar to those of wrought 1100 H14 aluminum. Microstructural examination and fractography clearly showed a change in fracture mechanism between the as-sprayed and annealed materials. These results indicate good potential for cold spray as a bulk-forming process.

**Keywords** aluminum, cold spray, heat treatment, mechanical properties, spray forming

## 1. Introduction

In the cold spray process, finely divided metal particles are accelerated in an inert gas jet to velocities in excess of 500 m/s. When accelerated to velocities above a material-dependent critical velocity,  $V_c$ , metal particles will bond to the substrate and form a dense, well-adhered deposit; this is the foundation of the cold spray process (Ref 1-3). The cold spray process is capable of preparing deposits of low-oxide content in air at near-room-temperature conditions. This makes cold spraying very attractive for many applications. Some of those applications, such as spray forming, require the cold-sprayed material to exhibit a modest amount of ductility. In their as-sprayed state, cold-sprayed metals tend to be brittle because the particles are heavily cold worked during the deposition process and interparticle bonding tends to be incomplete. The goal of this work was to better understand the factors affecting the ductility of cold-sprayed aluminum deposits. This will allow new applications for cold spray processing such as spray forming.

The original version of this paper was published in the CD ROM *Thermal Spray Connects: Explore Its Surfacing Potential*, International Thermal Spray Conference, sponsored by DVS, ASM International, and IIW International Institute of Welding, Basel, Switzerland, May 2-4, 2005, DVS-Verlag GmbH, Düsseldorf, Germany.

A.C. Hall, D.J. Cook, R.A. Neiser, and T.J. Roemer, Sandia National Laboratories, P.O. Box 5800, MS 1130, Albuquerque, NM 87123-1130; and D.A. Hirschfeld, New Mexico Institute of Mining and Technology, Department of Materials and Metallurgical Engineering, 801 Leroy Place, Socorro, NM 87801. Contact e-mail: achall@sandia.gov.

## 2. Experimental Procedure

Three different gas-atomized aluminum powders were investigated in this study: Valimet (Stockton, CA) H-10; Valimet H-20; and F.J. Brodmann (Harvey, LA) Flomaster powder. The H-10 powder had a volumetric mean particle size of 11.8  $\mu\text{m}$ . The H-20 and Brodmann powders had mean sizes of 25.9 and 26.4  $\mu\text{m}$ , respectively. Particle size distributions for each powder are shown in Fig. 1. All three powders were cold sprayed using a cold spray system that was designed and built by Ktech Corporation (Albuquerque, NM). The cold spray nozzle had a 2.0 mm diameter throat, a 100 mm long supersonic region, and a 5 mm diameter exit orifice. Helium was used as the accelerating gas. All samples were prepared using a raster speed of 100 mm/s and a standoff distance of 38 mm. The H-10 powder was sprayed using a 1723 kPa 350 °C accelerating gas flow. The calculated average centerline velocity for the H-10 powder at these conditions was 1117 m/s. The H-20 powder was sprayed using a 2240 kPa, 375 °C accelerating gas flow. The H-20 velocity was calculated as 880 m/s. The Flomaster powder was sprayed using a 1551 kPa, 400 °C accelerating gas flow. The calculated average centerline velocity for the Flomaster powder was 871 m/s. In all cases, the powder feed gas pressure was 5% higher than the accelerating gas pressure. The smaller size of the particles of the H-10 powder resulted in its velocity being substantially higher than those of the other two powders.

Spray deposits measuring 100  $\times$  100  $\times$  13 mm were laid down using a simple X-Y raster pattern. Tensile bars were machined from the as-sprayed deposits according to a modified ASTM E8 (Ref 4) geometry. The gage diameter of these samples was reduced from its normal value of 6.35 to 4.57 mm because the 6.35 mm gage diameter is so close to the root diameter of the 5/16 in.,

24 unified national fine (UNF) thread that the as-sprayed tensile samples were fracturing in the threads. Tensile bars were wrapped in aluminum foil then annealed at 300 °C for 22 h in air. A total of 27 tensile bars were tested. They were grouped as follows: H-20 as-sprayed, 8 bars; Flomaster as-sprayed, 6 bars; H-10 as-sprayed, 5 bars; H-20 annealed, 4 bars; Flomaster annealed, 2 bars; H-10 annealed, 2 bars.

The microstructures, fracture surfaces, and cross sections near the fracture of both the as-sprayed and annealed bars were examined using optical and scanning electron microscopy (SEM). Kikuchi mapping of the Valimet H-10 material in the as-sprayed and annealed conditions has also been conducted. Kikuchi mapping allows the indexing of grains, the identifica-

tion of grain boundaries, and phase identification using back-scattered diffraction patterns in an SEM image (Ref 5).

### 3. Results and Discussion

Optical micrographs of the as-sprayed deposits showed that the H-10 and H-20 powders produced deposits having densities >99.9%, while the Brodmann powder produced a more porous deposit with less particle deformation (Fig. 2). There was no optical evidence of grain growth in the annealed microstructures (Fig. 3).

In the as-sprayed condition, all three powders exhibited

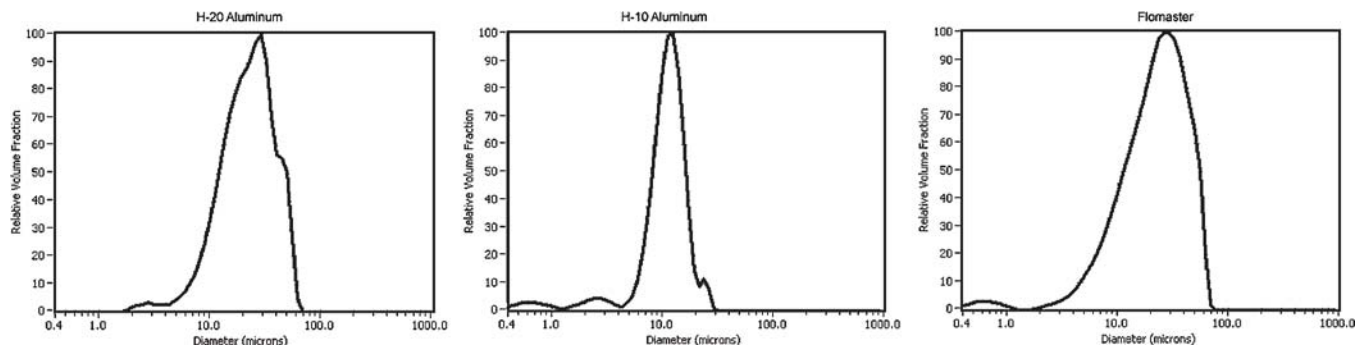


Fig. 1 Particle size distributions for H-10, H-20, and Flomaster powders

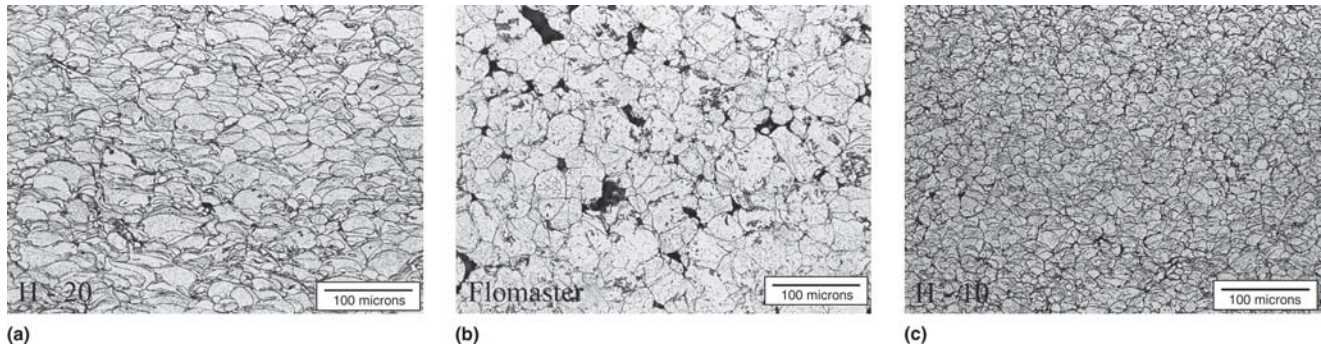


Fig. 2 As-sprayed cold spray aluminum deposits: (a) H-20; (b) Flomaster; (c) H-10

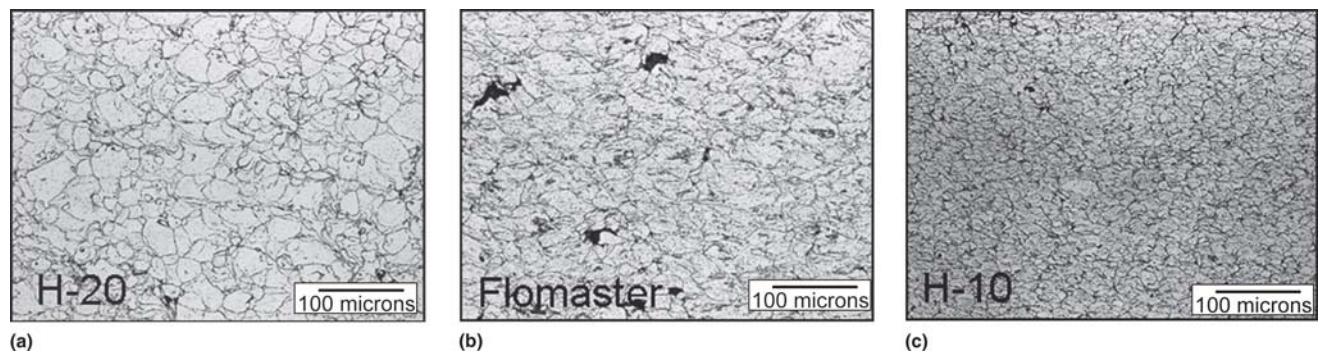


Fig. 3 Annealed cold spray aluminum deposits: (a) H-20; (b) Flomaster; (c) H-10

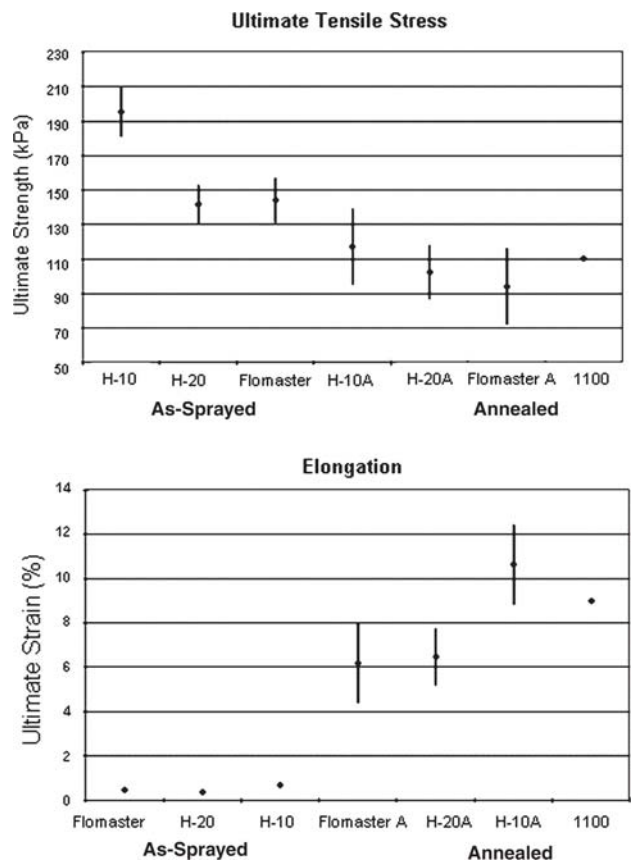


Fig. 4 Mechanical properties exhibited by tensile bars machined from H-10, H-20, and Flomaster cold spray deposits

brittle behavior; however, after annealing, they exhibited ductile behavior and mechanical properties that were similar to those of wrought aluminum. The H-20 and Flomaster deposits exhibited strains to failure of only ~0.4%, and the H-10 deposits a maximum of 1%. After annealing, the ductility increased by about a factor of 10. The mechanical properties of the annealed samples compares favorably with 1100 H14, a typical wrought aluminum. The as-sprayed ultimate tensile strength was higher than that of the annealed samples. It is believed that the H-10 samples exhibited greater elongation due to the finer particle size and higher density as a result of higher particle velocity. There was no significant difference in the elastic modulus for all samples. The observed mechanical properties are shown and compare favorably to those of 1100 H14 (Ref 6) (Fig. 4, 5).

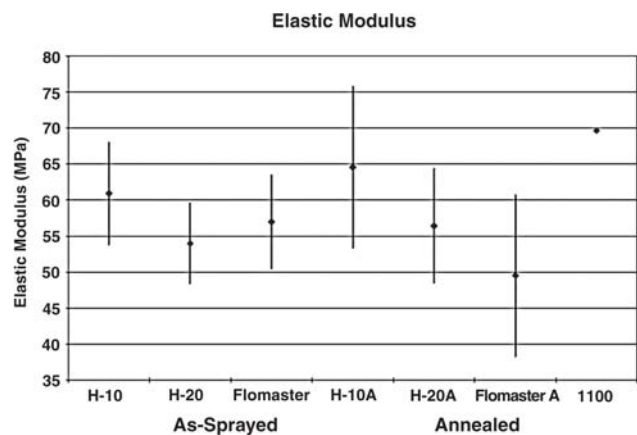


Fig. 5 Elastic modulus exhibited by tensile bars machined from H-10, H-20, and Flomaster cold spray deposits

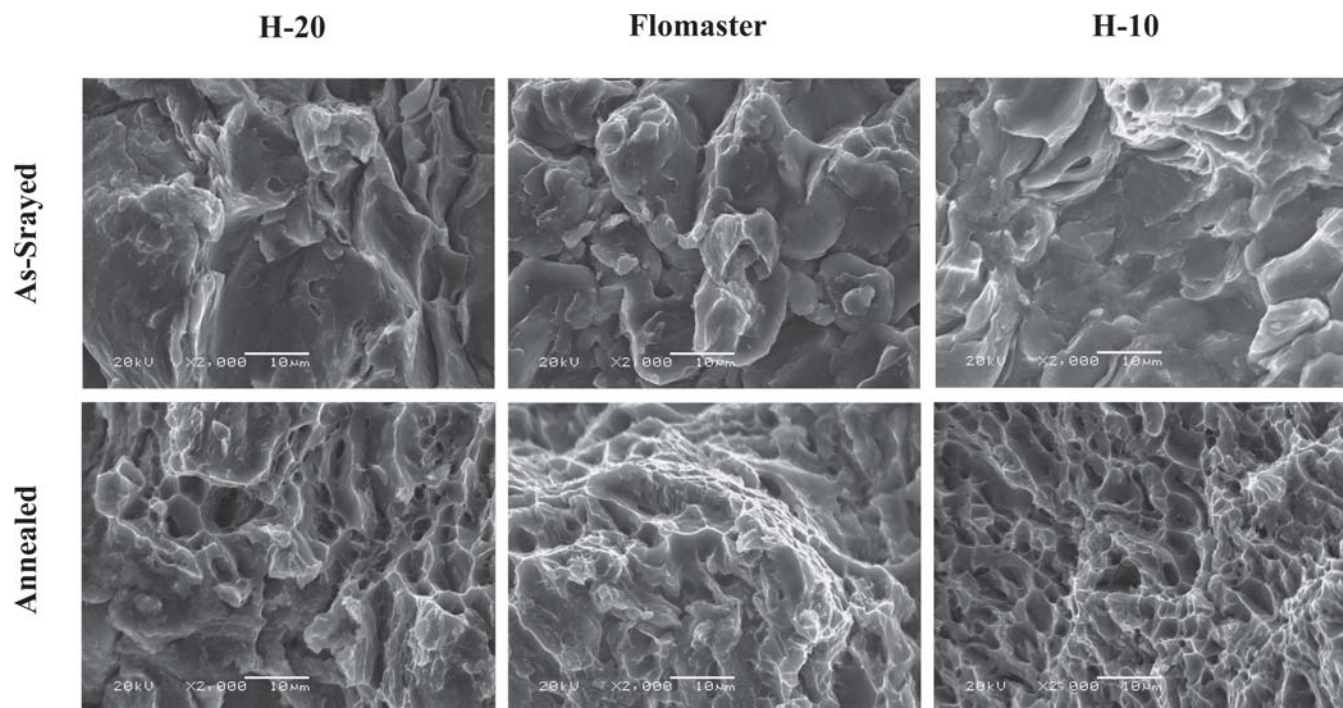
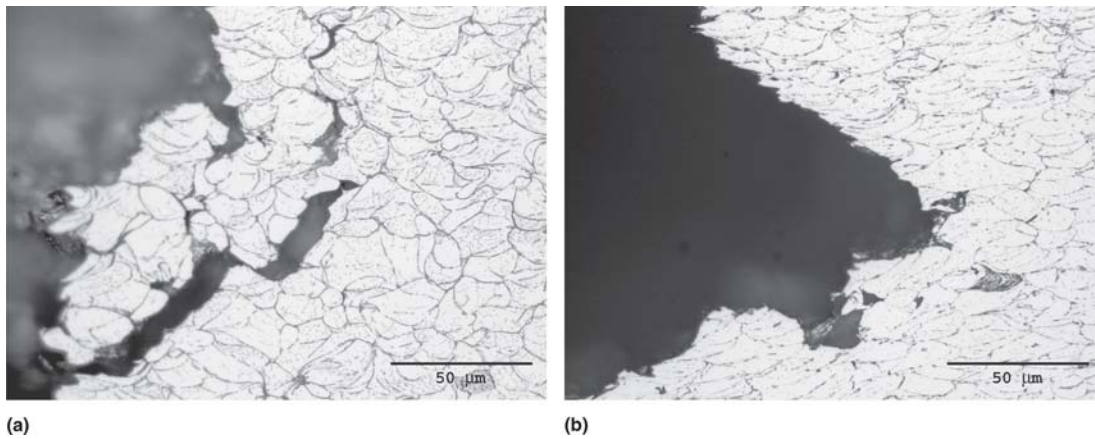


Fig. 6 The SEM micrographs of as-sprayed and annealed fracture surfaces



**Fig. 7** Metallographic section through the fracture surface of (a) as-sprayed and (b) annealed H-10 tensile bars

The fracture surfaces of the annealed deposits revealed features that are consistent with the observed increase in ductility. The as-sprayed samples exhibit brittle failure with a relatively smooth and blocky fracture surface. The annealed fracture surfaces are typical of ductile failure showing classic microvoid coalescence (Fig. 6).

Metallographic sections taken through the fracture region reveal that the as-sprayed specimens exhibited primarily brittle intragranular failure. This suggests incomplete bonding between splats during the cold spray deposition process. The H-10 specimen, which has almost twice the elongation of the H-20 or Flo-master specimens, exhibited some transgranular failure. Micrographs of the annealed sections showed considerable elongation and flow of the individual grains. The fracture appears to be of a mixed mode with intergranular failure and a large amount of void-coalescence, which is typical of ductile fracture (Fig. 7).

Kikuchi maps (Ref 4) were prepared in the grip section of both the as-sprayed and annealed tensile bars (Fig. 8, 9). The grip sections of the tensile bars were analyzed to ensure that deformation from the tensile test did not confound the results.

Figures 8 and 9 show grain orientation as color maps. Black regions indicate areas where the SEM system was not able to index the Kikuchi pattern due to low contrast. Typically, this results from the presence of voids (porosity) or very small grains. Figure 10 is an index to the color mapping shown in Fig. 8 and 9. Grain orientation is referenced with respect to the beam direction.

Analysis of the data presented in Fig. 11 and 12 shows the location of high-angle and low-angle grain boundaries.

These data clearly show that the as-sprayed H-10 material contains significantly more high-angle grain boundaries than the annealed material. The grains in the as-sprayed coating are 1 to 5  $\mu\text{m}$  in size. This is significantly smaller than the mean initial powder particle size of 11.8  $\mu\text{m}$ . The small grain size in this material is due to the high deformation associated with the cold spray process. The size and shape of the grains in the annealed material suggest that their boundaries are associated with the splat boundaries. It is also clear that the as-sprayed material contains significantly more low-angle grain boundaries than the annealed material. This demonstrates that the aluminum crystals in the as-sprayed material have a higher dislocation density than

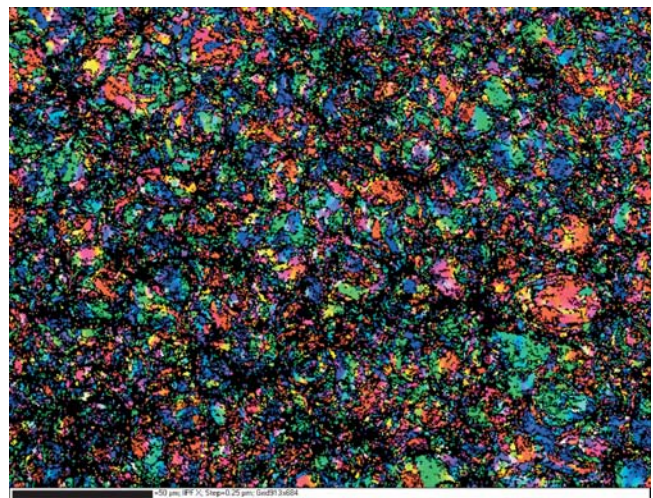


**Fig. 8** Kikuchi map of the as-sprayed H-10 material. Scale bar is 50  $\mu\text{m}$ .

the crystals in the annealed material. Clearly, significant recrystallization and associated dislocation recovery have occurred in the annealed material. Interestingly, significant grain growth beyond the splat boundaries does not appear to have occurred in the annealed material. The SEM images of the polished sample surface show this (Fig. 13, 14). Figure 13 shows the polished surface of the as-sprayed sample, and the annealed sample is shown in Fig. 14. Porosity at the splat boundaries can be seen clearly in both the as-sprayed and annealed samples. This porosity is consistent with the idea that the consolidation of cold-sprayed material occurs through a partial metallurgical bonding between the splats. Interestingly, the porosity along the splat boundaries does not appear to be significantly different when the as-sprayed and annealed samples are compared. This observation, combined with a lack of grain growth across the splat boundaries, indicates that the splat boundaries have not changed significantly as a result of annealing.

The data shown above explain the change in the fracture mechanism and the increase in ductility observed upon annealing. Recrystallization and reduction of the dislocation density of

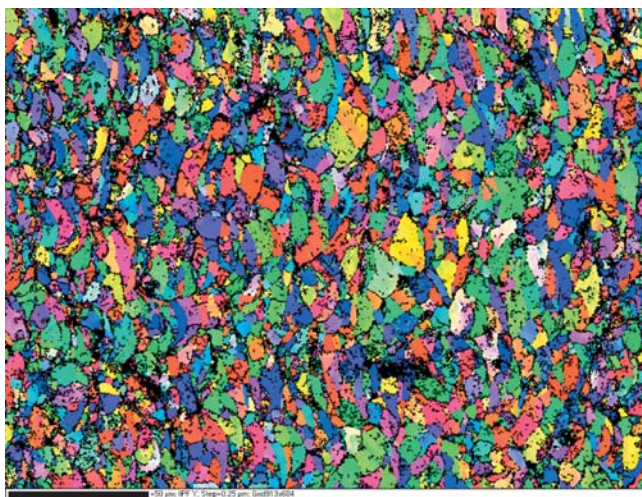


**Fig. 9** Kikuchi map of the annealed H-10 cold-sprayed material. Scale bar is 50  $\mu\text{m}$ .

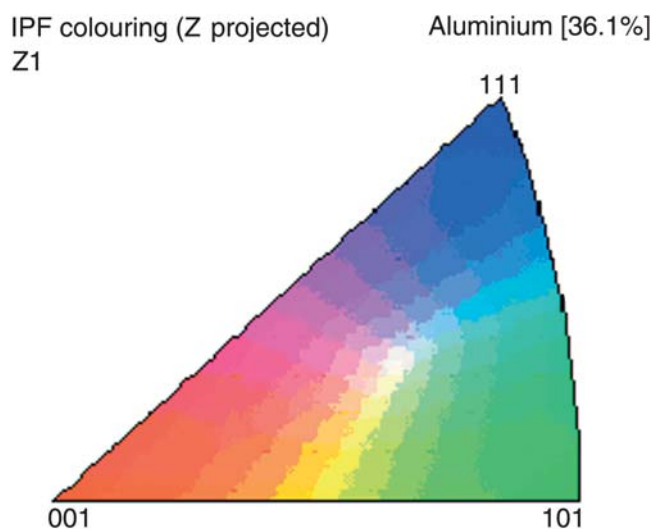


**Fig. 10** Index to Fig. 8 and 9. The orientation is referenced with respect to the beam direction.

the aluminum material occurred within the splats during the anneal, resulting in increased ductility and decreased strength. No macroscopic changes in the splat boundaries were observed upon annealing. Clearly, the orientation relationships along the splat boundaries changed as recrystallization occurred within the splats, but no coarsening of the material structure beyond the splat boundaries was observed. Thus, only recrystallization within the splats and a reduction in dislocation density in the aluminum crystals can be responsible for the observed changes in the mechanical properties and fracture mechanism.

#### 4. Conclusions

- Annealed cold spray deposits  $\sim 1$  cm thick exhibit elastic moduli, ultimate tensile strength, and elongations similar to

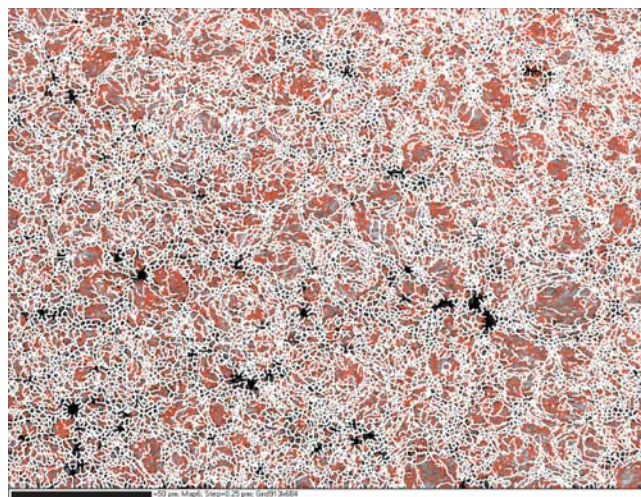


**Fig. 11** High-angle grain boundaries ( $>10^\circ$ ), shown in white, and low-angle grain boundaries ( $<3^\circ$ ), shown in red, for the as-sprayed H-10 aluminum. Scale bar is 50  $\mu\text{m}$ .

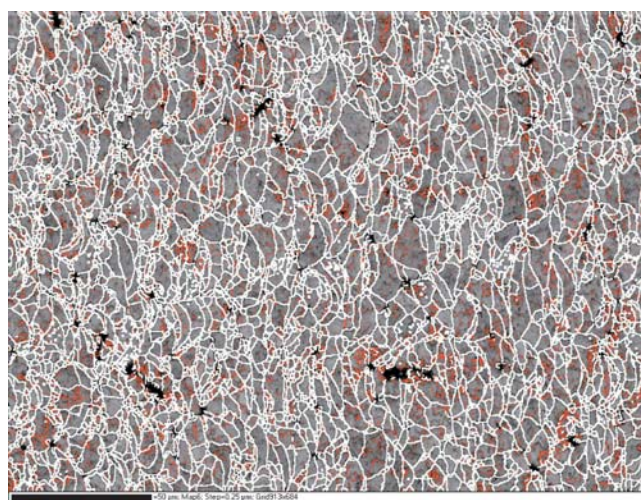


**Fig. 12** High-angle grain boundaries ( $>10^\circ$ ), shown in white, and low-angle grain boundaries ( $<3^\circ$ ), shown in red, for the annealed H-10 aluminum. Scale bar is 50  $\mu\text{m}$ .

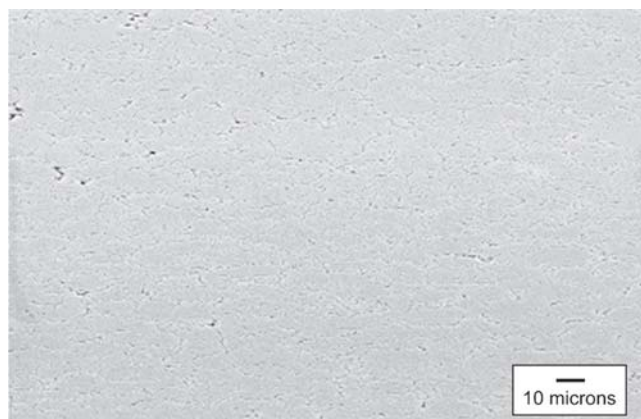


**Fig. 13** An SEM micrograph showing the polished surface of the as-sprayed material. Porosity can be seen along the splat boundaries.

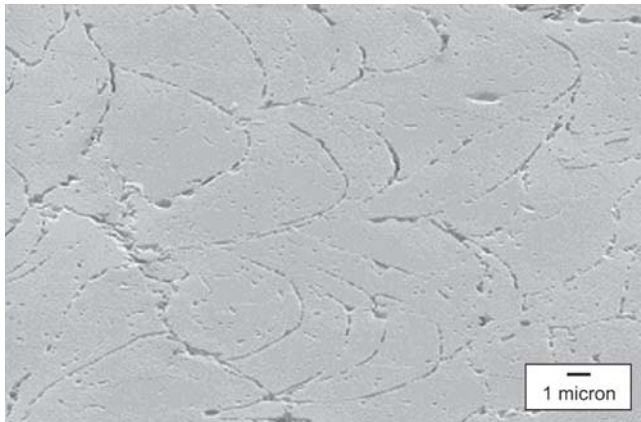


**Fig. 14** An SEM micrograph showing the polished surface of the annealed material. Porosity can be seen along the splat boundaries. Note: this image has a higher magnification than Fig. 13.

those of wrought aluminum. This indicates that the cold spray technology may be used for the spray forming of aluminum components.

- The primary mechanism for mechanical property changes in commercially pure cold spray deposits exposed to a moderate anneal is the reduction in dislocation density within the aluminum splats.

- Finer aluminum powder sizes that yield higher particle velocities also yield higher density deposits, which results in increased ductility compared with coarser powders. This was observed for both as-sprayed and annealed deposits.

### Acknowledgments

Sandia is a multiprogram laboratory operated by Sandia Corporation, a Lockheed Martin Company, for the U.S. Department of Energy under contract No. DE-AC04-94-AL85000.

### References

1. M.F. Smith, J.E. Brockmann, R.C. Dykhuizen, D.L. Gilmore, R.A. Neiser, and T.J. Roemer, Cold Spray Direct Fabrication-High Rate Solid State, Material Consolidation, *Mater. Res. Soc. Symp. Proc.*, 1999, **542**, p 65-76
2. D.L. Gilmore, R.C. Dykhuizen, R.A. Neiser, T.J. Roemer, and M.F. Smith, Particle Velocity and Deposition Efficiency in the Cold Spray Process, *J. Thermal Spray Technol.*, 1999, **8**(4), p 576-582
3. R.C. Dykhuizen, M.F. Smith, D.L. Gilmore, R.A. Neiser, X. Jiang, and S. Sampath, Impact of High Velocity Cold Spray Particles, *J. Thermal Spray Technol.*, 1999, **8**(4), p 559-564
4. "Standard Test Methods for Tension Testing of Metallic Materials," E8-04, *Annual Book of ASTM Standards*, ASTM, 2004
5. J.R. Michael and R.P. Goehner, Electron Backscatter Diffraction: A Powerful Tool for Phase Identification in the SEM, *Materials Research Society Fall Meeting* Nov 29-Dec 3 (Boston, MA), 1999
6. Physical Metallurgy of Aluminum Alloys, *Metals Handbook*, Desk Edition, 2nd ed., J.R. Davis, Ed., ASM International, 1998, p 462